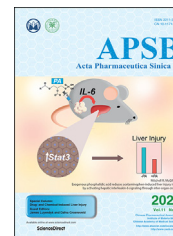




Chinese Pharmaceutical Association
Institute of Materia Medica, Chinese Academy of Medical Sciences

Acta Pharmaceutica Sinica B

www.elsevier.com/locate/apsb
www.sciencedirect.com



ORIGINAL ARTICLE

Altered cisplatin pharmacokinetics during nonalcoholic steatohepatitis contributes to reduced nephrotoxicity



Joseph L. Jilek^a, Kayla L. Frost^a,
Kevyn A. Jacobus^a, Wenxi He^a, Erica L. Toth^a,
Michael Goedken^b, Nathan J. Cherrington^{a,*}

^aDepartment of Pharmacology & Toxicology, College of Pharmacy, University of Arizona, Tucson, AZ 85724, USA

^bRutgers Translational Sciences, Rutgers University, Piscataway, NJ 08901, USA

Received 16 December 2020; received in revised form 9 March 2021; accepted 15 April 2021

KEY WORDS

Nonalcoholic
steatohepatitis;
NASH;
Cisplatin;
Drug transporter;
Nephrotoxicity

Abstract Disease-mediated alterations to drug disposition constitute a significant source of adverse drug reactions. Cisplatin (CDDP) elicits nephrotoxicity due to exposure in proximal tubule cells during renal secretion. Alterations to renal drug transporter expression have been discovered during nonalcoholic steatohepatitis (NASH), however, associated changes to substrate toxicity is unknown. To test this, a methionine- and choline-deficient diet-induced rat model was used to evaluate NASH-associated changes to CDDP pharmacokinetics, transporter expression, and toxicity. NASH rats administered CDDP (6 mg/kg, i.p.) displayed 20% less nephrotoxicity than healthy rats. Likewise, CDDP renal clearance decreased in NASH rats from 7.39 to 3.83 mL/min, renal secretion decreased from 6.23 to 2.80 mL/min, and renal CDDP accumulation decreased by 15%, relative to healthy rats. Renal copper transporter-1 expression decreased, and organic cation transporter-2 and ATPase copper transporting protein-7b increased slightly, reducing CDDP secretion. Hepatic CDDP accumulation increased 250% in NASH rats relative to healthy rats. Hepatic organic cation transporter-1 induction and multidrug and toxin extrusion protein-1 and multidrug resistance-associated protein-4 reduction may contribute to hepatic CDDP sequestration in NASH rats, although no drug-related toxicity was observed. These data

Abbreviations: ATP7, ATPase copper transporting protein; CDDP, cisplatin; CTR, copper transporter; DDTC, diethyldithiocarbamate; DT, drug transporter; GFR, glomerular filtration rate; LC–MS/MS, liquid chromatography–tandem mass spectrometry; MATE, multidrug and toxin extrusion protein; MCD, methionine- and choline-deficient diet; NAFLD, nonalcoholic fatty liver disease; NASH, nonalcoholic steatohepatitis; OCT, organic cation transporter; P-gp, p-glycoprotein; PK, pharmacokinetics.

*Corresponding author. Tel.: +1 520 626 0219.

E-mail address: cherrington@pharmacy.arizona.edu (Nathan J. Cherrington).

Peer review under responsibility of Chinese Pharmaceutical Association and Institute of Materia Medica, Chinese Academy of Medical Sciences.

<https://doi.org/10.1016/j.apsb.2021.05.030>

2211-3835 © 2021 Chinese Pharmaceutical Association and Institute of Materia Medica, Chinese Academy of Medical Sciences. Production and hosting by Elsevier B.V. This is an open access article under the CC BY-NC-ND license (<http://creativecommons.org/licenses/by-nc-nd/4.0/>).

provide a link between NASH-induced hepatic and renal transporter expression changes and CDDP renal clearance, which may alter nephrotoxicity.

© 2021 Chinese Pharmaceutical Association and Institute of Materia Medica, Chinese Academy of Medical Sciences. Production and hosting by Elsevier B.V. This is an open access article under the CC BY-NC-ND license (<http://creativecommons.org/licenses/by-nc-nd/4.0/>).

1. Introduction

Cis-Diaminedichloridoplatinum (II) (cisplatin, CDDP) is a first-generation platinum-based antineoplastic indicated for many solid tumors¹. Proliferating cells are primarily killed by CDDP as a result of DNA crosslinking leading to stalled replication. As a cytotoxic antineoplastic agent, healthy tissues are also susceptible to CDDP toxicity, leading to dose limiting toxicity¹. Under physiological pH, CDDP is uncharged, although its pharmacokinetics (PK) is heavily dependent on organic cation transporters, as well as clearance by enzymatic conjugation. As such, tissues expressing organic cation transporters (OCT1-3), as well as copper transporter 1 (CTR1) accumulate CDDP at rates higher than other tissues and are subsequently more sensitive to toxicity^{2–4}. This leads to selective CDDP-mediated nephrotoxicity and ototoxicity. Additionally, glutathione conjugation of CDDP to a toxic metabolite may explain regiospecific CDDP toxicity within region III of the proximal convoluted tubule^{5–8}. Efflux of CDDP from renal proximal tubule cells is highly dependent on multidrug and toxin extrusion protein (MATE) isoforms, of which MATE1 is predominantly expressed in the rat kidney⁹. Likewise, reduced MATE1/2 and/or increased OCT2 expression, the predominant isoform in the kidney, is a key indicator of CDDP toxicity¹⁰. Finally, renal cell efflux and reabsorption of CDDP and its metabolites by multidrug resistance-associated proteins (MRP) may also contribute to selective CDDP toxicity in the proximal convoluted tubules¹¹.

Growing evidence suggests that metabolic diseases elicit systemic changes to physiological processes, including drug transporters¹². Indeed, non-genetic alterations in protein expression and function during disease progression (known as phenoconversion) is a significant contributor to pharmacogenomic variability, especially in the liver¹³. This is an emerging issue specifically for nonalcoholic fatty liver disease (NAFLD) and nonalcoholic steatohepatitis (NASH), the progressive and irreversible form of NAFLD^{14–16}. Given the rising prevalence of NASH, understanding this source of population variation in drug clearance and toxicity is timely. Evidence of hepatic phenoconversion of drug transporters during NASH is well documented and causes subsequent changes to drug disposition and response^{17,18}. Recently, extrahepatic changes to expression of specific drug transporters in rodent models of NASH have been identified; this includes increased P-glycoprotein (P-gp) and MRP2 expression, although considerable variability exists between models¹⁴. Additionally, glomerular filtration rate (GFR) in both human NASH patients and rodent models of NASH is significantly reduced, further altering renal clearance of many drugs¹².

Variability in CDDP nephrotoxicity is a significant concern, as this often limits treatment options and can be acutely life threatening. Although second and third generation platinating agents with reduced nephrotoxicity have been developed, their therapeutic efficacy may be reduced or compromised in resistant tumors, promoting the continued clinical utility of CDDP. Interestingly, circadian regulation of OCT2 and MATE1 in rodent, which can

uptake and efflux CDDP, respectively, influences renal CDDP clearance and subsequent toxicity, further demonstrating that renal CDDP flux alters nephrotoxicity¹⁹. While OCT and MATE transporter expression changes are characterized in terms of differential disposition and toxicity, collective changes to the expression of all CDDP transporters is less understood. As such, the current study aims to characterize CDDP nephrotoxicity, considering NASH-induced changes to drug transporters of the entire kidney using a surrogate peptide LC–MS/MS (liquid chromatography–tandem mass spectrometry) method. Herein, we utilized rats fed a methionine- and choline-deficient (MCD) diet to induce NASH to evaluate the impact of the disease on CDDP PK, renal disposition, and nephrotoxicity. The data presented in this study suggest that, in NASH rats, a reduction in renal clearance and disposition of CDDP contributes to a reduction in associated nephrotoxicity.

2. Materials and methods

2.1. Chemicals and reagents

CDDP, diethyldithiocarbamate (DDTC), 8-cyclopentyl-1,3-dipropylxanthine (DPCPX), dithiothreitol, and sodium deoxycholate were purchased from Sigma–Aldrich (St. Louis, MO, USA). LC–MS/MS grade water, methanol, and acetonitrile were purchased from Fisher Scientific (Pittsburgh, PA, USA). Iohexol was purchased from TCI, Inc. (Portland, OR, USA). Protease inhibitor cocktail was purchased from Thermo Scientific (Rockford, IL, USA). Phenylmethylsulfonyl fluoride (PMSF) was purchased from MP Biomedicals (Solon, OH, USA). Ammonium bicarbonate was purchased from Oakwood Chemical (Estill, SC, USA). Iodoacetamide was purchased from Biorad (Hercules, CA, USA).

2.2. Animal use and NASH induction

All procedures involving live rats were approved by the University of Arizona Institutional Animal Care and Use Committee; husbandry and veterinary care were provided by trained animal care staff. Eight-week old male Sprague–Dawley rats were purchased from Charles River Laboratories (Hollister, CA, USA) and housed two per cage in 12 h on/off light cycles. Control and MCD rodent diets were purchased from Dyets, Inc. (Bethlehem, PA, USA). Rats were given water and either control or MCD diet (to induce NASH) *ad libitum* for 8 weeks. Following experimental procedures, rats were euthanized by carbon dioxide overdose and exsanguination. To allow for sufficient sample collection timing, CDDP dosing was administered in all animals at Zeitgeber time 2 ± 30 min.

2.3. In vivo CDDP toxicity and disposition

To evaluate CDDP toxicity in healthy and NASH rats, six rats from each diet were administered a bolus 6 mg/kg CDDP i.p.

(1 mg/mL in sterile saline); this dose has been shown to elicit nephrotoxicity without gross systemic toxicity in rats²⁰. Another six rats from each diet were administered vehicle (saline) i.p. as a drug-naïve cohort. After 72 h at Zeitgeber time 2 ± 30 min, animals were euthanized by carbon dioxide overdose and liver and kidney were harvested. A portion of each tissue was fixed in neutral-buffered formalin, dehydrated, and embedded into paraffin blocks for hematoxylin and eosin (H&E)-staining. Hepatic and renal toxicity was scored by a board-certified veterinary pathologist as previously described¹⁵. To evaluate CDDP disposition in healthy and NASH rats, a separate cohort of six rats from each diet were administered 6 mg/kg CDDP i.p. ($t = 0$). Approximately 100 μ L of blood was collected following dosing (Zeitgeber time 2 ± 30 min) at 5, 10, 30, 45, 90, 120, 180, 240, 300, and 360 min post-dose from the lateral tail vein. Urine was collected at the same intervals in a metabolic cage. Simultaneously, to determine glomerular filtration rate (GFR), 25 mg/kg iohexol in sterile saline was administered by tail vein injection at $t = 0$. At $t = 360$ min, rats were euthanized by carbon dioxide overdose and liver and kidneys were harvested and snap-frozen to determine tissue disposition and transporter expression.

2.4. LC-MS/MS quantification of CDDP

Following collection, blood was transferred to heparinized tubes and centrifuged at $2000 \times g$ for 10 min at 4°C . The plasma and urine were frozen and stored at -80°C prior to use. Approximately 150 mg of snap-frozen liver and kidney tissue were homogenized with a rotary tissue grinder in 80:20 methanol/water containing internal standard (DPCPX) at a constant ratio of 1 ng DPCPX to 100 mg tissue. Calibrators were prepared in a similar manner with CDDP spiked in to homogenized tissue and serially diluted (Table 1).

All biological matrices (plasma, urine, and tissues) were derivatized with DDTC, adapted from the work of Shaik et al²¹. Briefly, an aliquot of sample or calibrator (45 μ L urine, 10 μ L plasma, or 500 μ L tissue homogenate) was added to 15 μ L (urine), 5 μ L (blood), or 125 μ L (tissue homogenate) of DDTC (1%, w/v) in 0.1 mol/L NaOH and incubated for 30 min at 40°C . To quench the reaction, 1 mL acetonitrile was added with DPCPX at 10 ng/mL (urine) or 0.5 ng/mL (blood) and centrifuged at $3000 \times g$ for 10 min.

The supernatant was collected, evaporated over air, and reconstituted in 40:60 acetonitrile/water with 0.1% formic acid (200 μ L for urine and blood, 100 μ L for tissue homogenate). Derivatized CDDP and IS were separated on a Luna[®] Omega Polar C18 column (50 mm \times 2.1 mm, 1.6 μ m particle diameter) using a Shimadzu LC-20AD liquid chromatography system. Both analytes were separated using a binary flow (0.2 mL/min) gradient consisting of water/0.1% formic acid (mobile phase A) and acetonitrile/0.1% formic acid (mobile phase B) as follows: 40% B (0–0.5 min), 40%–75% B (0.5–0.75 min), 75%–90% B (0.75–1.25 min), 90%–95% B (1.25–2.25 min), 95% B (2.25–3.75 min), 95%–40% B (3.75–4.5 min), and re-equilibration at 40% B for 1.5 min. Both analytes were detected using a Sciex QTrap[®] 4500+ triple quadrupole tandem mass spectrometer operated in positive electrospray ionization with the following source parameters: 4.5 kV ionspray voltage, 450°C source temperature, 20 psi curtain gas, 9 psi collision gas, 20 psi nebulizer gas, and 40 psi turbo gas. Derivatized CDDP (492.0 \rightarrow 425.5) and IS (305.0 \rightarrow 178.0) were detected by multiple reaction monitoring with the following parameters: 90 V declustering potential, 10 V entrance potential, 30 eV collision energy, 10 V collision cell exit potential; collision energy values for derivatized CDDP and IS were 25 and 33 eV, respectively.

2.5. Glomerular filtration rate determined by iohexol clearance

Iohexol plasma clearance was determined to calculate GFR as adapted from the work of Ref. 22. Briefly, 5 μ L of plasma already collected at $t = 30, 90,$ and 360 min was spiked with 1 mL of 5 ng/mL d_5 -iohexol (internal standard), vortexed briefly, and centrifuged at $2000 \times g$ for 30 min at 4°C . Eight-hundred microliters of supernatant were transferred to clean tubes and dried over air. The residue containing all analytes was reconstituted in 100 μ L of 95:5 water/acetonitrile with 0.1% formic acid and two μ L was injected onto a Luna[®] Omega Polar C18 column (50 mm \times 2.1 mm, 1.6 μ m particle diameter) using a Shimadzu LC-20AD liquid chromatography system. Iohexol and d_6 -iohexol were separated using a binary flow gradient (0.25 mL/min) with water/0.1% formic acid (mobile phase A) and acetonitrile/0.1% formic acid (mobile phase B) as follows: 5% B (0–3.5 min), 5%–80% B (1–3.5 min), 80% B (3.5–4.5 min), 80%–5% B (4.5–5 min), and re-equilibration at 5% B for 1.5 min. Both

Table 1 Surrogate peptides used to quantify protein expression and MRM transitions used for LC-MS/MS detection in this study.

Protein	Peptide sequence	IS	RT (min)	Q1 [M+2H] ²⁺ (Da)	Q3 [M+H] ⁺ (Da)
ATP7A	LGAI DVER	MRP2-H	12.8	436.7	759.4
ATP7B	AIATQV GINK	MRP2-H	11.4	507.8	759.4
CTR1	SQVSIR	MRP2-H	7.9	345.2	474.3
MRP2	GINLSGGQK	MRP2-H	10.0	437.2	703.4
MRP4	APVLF FDR	MRP4-H	20.2	482.8	697.4
MATE1	HVG VILQR	MRP4-H	11.4	461.3	685.4
OCT1	VPPADLK	MRP2-H	9.0	370.2	640.4
OCT2	FLQGLVSK	OCT2-H	16.1	446.3	503.3
OCT3	TTVATLGR	MRP2-H	10.3	409.7	616.4
P-gp	IATEAIENFR	OCT2-H	15.8	582.3	979.5
MRP2-H	GINL*SGGQK	—	10.0	440.7	710.4
MRP4-H	APVL*FFDR	—	20.2	486.3	704.4
OCT2-H	FLQGL*VSK	—	16.1	449.8	751.5

Membrane protein fractions were digested with trypsin per *Materials and Methods* to quantify transporter expression. Multiple reaction monitoring transitions used for detection are listed as doubly-charged parent ion (Q1) and singly charged fragment ion (Q3) used for quantification. ¹³C/¹⁶N heavy isotope labeled amino acid internal standards (IS). RT, retention time for liquid chromatography method. —Not applicable.

analytes were detected using a Sciex QTrap® 4500+ mass spectrometer in positive electrospray ionization as detailed above. Iohexol (821.7 → 803.6) and *d*₆-iohexol (826.7 → 808.7) were detected by multiple reaction monitoring with the following parameters: 100 V declustering potential, 10 V entrance potential, 30 eV collision energy, 15 V collision cell exit potential.

Both analytes were integrated and iohexol was normalized and quantified against *d*₆-iohexol using Analyst MultiQuant™ software. Plasma iohexol clearance was measured by non-compartmental analysis using the AUC method (CL = AUC_{0-∞}/Dose) and used as a surrogate for GFR.

2.6. Transporter expression analysis by surrogate peptide LC-MS/MS

To evaluate membrane transporter expression in liver and kidney tissue, approximately 100 mg of snap-frozen tissue were homogenized in a Potter-Elvehjem homogenizer over ice (approximately 20 strokes) in 100 mmol/L Tris-HCl (pH 7.4), 100 mmol/L NaCl, 1.5 mmol/L MgCl₂, 1 mmol/L PMSF, and 1 × protease inhibitor cocktail (Pierce). The homogenate was centrifuged at 8000×*g* for 10 min at 4 °C to remove debris and the S9 fraction (supernatant) was further centrifuged at 100,000×*g* for 1 h at 4 °C to pellet the membrane fraction which was reconstituted with 10 mmol/L Tris-HCl (pH 8.0). A 300 μg aliquot was diluted into 100 mmol/L ammonium bicarbonate with 3.7% sodium deoxycholate (*w/v*). Proteins were denatured at 95 °C for 5 min with 6 mmol/L dithiothreitol and then alkylated with 15 mmol/L iodoacetamide for 20 min at room temperature in the dark. The alkylation reaction was quenched by the addition of 20 mmol/L dithiothreitol and proteins were digested at 37 °C overnight with sequencing-grade trypsin (Promega) at an enzyme/substrate ratio of 1:100. The digestion reaction was quenched by acidifying the solution with formic acid to 0.4% with a cocktail of heavy-labeled internal standard peptides (0.2 ng/sample) per Table 1. Peptide samples were then centrifuged at 20,000×*g* for 15 min at 4 °C and the supernatants containing peptides were cleaned up by strong-anion exchange solid phase extraction cartridges (Waters, Inc.) as follows: 1 mL methanol (conditioning), two mL water with 2% formic acid (equilibrating), sample application in 1 mL water with 2% formic acid, 1 mL water with 2% formic acid (washing), 0.2 mL water:acetonitrile 60:40 with 2% ammonium hydroxide (elution). Eluted peptides were dried with a speed-vac and reconstituted with 50 μL 95:5 water:acetonitrile with 0.1% formic acid. Ten microliters were injected onto a 2.1 mm × 100 mm Acquity UPLC® HSS C18 column (Waters) with 1.8 μm particles. The binary liquid chromatography gradient (mobile phase A: water+0.1% formic acid, mobile phase B: 90:10 acetonitrile/water+0.1% formic acid) was applied by an Agilent UPLC system as follows: 5.5% B (0–5 min), 5.5%–90% B (5–25 min), 90% B (25–26 min), 5.5% B (26–28 min). Surrogate peptides were detected with a Sciex QTrap 6500+ mass spectrometer operated in positive electrospray ionization set to the following parameters for all multiple reaction monitoring transitions: 500 °C source temperature, 20 psi curtain gas, 50 psi nebulizer gas, 25 psi turbo gas, 10 eV entrance potential, 50 V declustering potential, 25 V collision energy, and 15 V collision cell exit potential. MRM mass transitions for each surrogate peptide are listed in Table 1. Analyte peaks were quantified using MultiQuant (version 3, Sciex), quantified against the ratio of neat peptide standards divided by heavy-labeled internal standard peptides as indicated in Table 1; calibrators covered a range of

2–200 pmol pure surrogate peptide, based on on-column quantity. Absolute protein abundance was calculated by the following equation where “Surrogate Peptide” represents the on-column concentration quantified by LC-MS/MS and “Peptide Input” represents the total amount of peptide following digestion and solid phase extraction:

$$\text{Protein abundance (pmol / mg protein)} = \frac{[\text{Surrogate Peptide}](\text{pg})}{\text{MW (g/mol)}} \times \frac{1}{[\text{Peptide Input}](\text{mg})} \quad (1)$$

2.7. Data analysis

Pharmacokinetic parameters were derived by non-compartmental analysis (NCA) using the AUC_{0-∞} method to compute plasma volume of distribution (*V*) and clearance (CL). Renal clearance (CL_r) was determined over a 6 h interval as the fraction of cumulative CDDP in the urine divided by plasma AUC_{last}; renal secretion of CDDP was defined as the difference of GFR and CL_r. Protein abundance was quantified by total protein input and molecular weight of surrogate peptides detected by LC-MS/MS. Means were compared by either two-tailed Student's *t*-test or ANOVA where appropriate using Prism GraphPad (La Jolla, CA, USA).

3. Results

3.1. CDDP nephrotoxicity is reduced in NASH rats

To evaluate the effect of NASH on CDDP toxicity, NASH-induced and healthy rats were given either a bolus dose of 6 mg/kg CDDP (*i.p.*) or saline vehicle and were evaluated for gross and organ-specific pathology 72 h later. At sacrifice, healthy and NASH rats displayed no significant change in bodyweight relative to naïve rats. Furthermore, NASH-induced rats did not lose significantly more bodyweight over 72 h than healthy CDDP-treated rats (Fig. 1). CDDP induced significant increases in kidney weight of 31% and 22% in healthy and NASH rats, respectively; this difference in mean relative kidney mass gain was not significant when comparing CDDP-treated healthy and NASH rats (Fig. 1). Regardless, overall kidney pathological scoring was slightly but significantly reduced from 13.33 ± 1.51 to 10.60 ± 3.29 in NASH rats, relative to control rats (Table 2). Specifically, necrosis and inflammation decreased by approximately half in NASH rats (Table 2 and Fig. 2). Generally, CDDP caused mild to moderate degeneration of distal regions of the proximal convoluted tubule (Fig. 2, black arrows) and this was more prevalent in control than NASH rats.

As expected, liver mass increased by approximately 5 g/kg BW due to the MCD diet inducing NASH; confirmation of the NASH disease state was also verified by pathology in NASH rats (Table 3). Interestingly, a slight 10% reduction in liver mass approached significance (*P* = 0.06) in CDDP-treated healthy (Fig. 1), but not NASH rats, relative to naïve rats. However, CDDP-related histological alterations were found in liver tissue when comparing within disease groups of rats (Table 3).

3.2. Renal and plasma clearance of CDDP is attenuated during NASH

In a separate group of rats given a bolus dose of 6 mg/kg CDDP *i.p.*, plasma concentrations and total recovered urine CDDP were

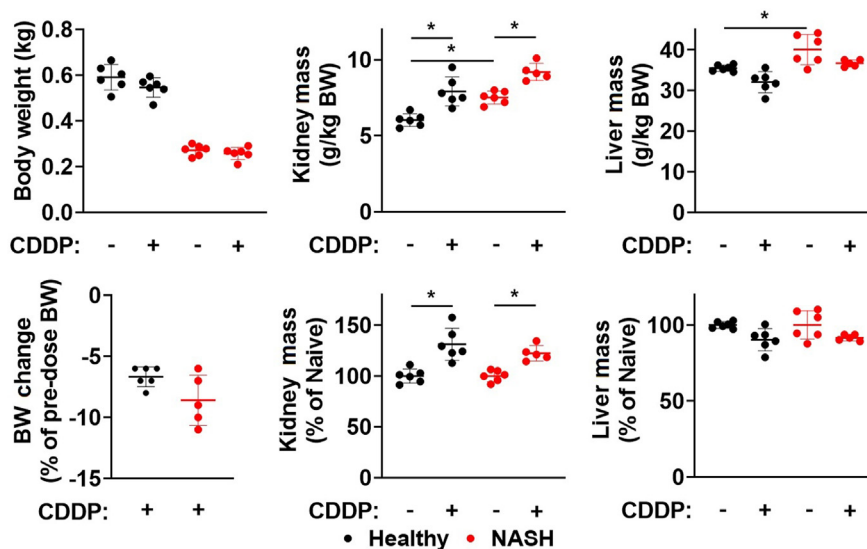


Figure 1 CDDP-treated rats display selective nephrotoxicity and is slightly reduced during NASH. Bolus-dosed healthy and NASH rats (6 mg/kg CDDP, i.p.) were sacrificed 3 days following treatment when body and organ weights were measured. Increased kidney mass (relative to drug naïve rats) and decreased body weight (relative to pre-dose) in CDDP-treated rats were consistent regardless of diet. Following CDDP treatment, a reduction in liver mass (relative to drug naïve rats) approached significance in healthy rats, but not in NASH rats. Scatter plots represent individual animals with mean values (horizontal lines) \pm standard deviation of $n = 6$ animals/group. Mean values were compared by two-way ANOVA with Sidak's *post-hoc* tests where $P < 0.05$ (*).

Table 2 Kidney histopathological scoring of healthy and NASH rats receiving either CDDP or vehicle.

Disease	Drug	Total	Degeneration	Necrosis	Apoptosis	Inflammation	Hyalin casts
Control	Naïve	0.50 \pm 1.22	0.33 \pm 0.82	0	0	0.17 \pm 0.41	0
	CDDP	13.33 \pm 1.51	3.17 \pm 0.75	4.00 \pm 0.89	1.17 \pm 0.41	2.17 \pm 0.41	2.83 \pm 0.75
NASH	Naïve	0	0	0	0	0	0
	CDDP	10.60 \pm 3.29	3.80 \pm 1.64	2.40 \pm 0.55	1.40 \pm 0.55	0.80 \pm 0.84	2.20 \pm 0.84
Two-way ANOVA	Diet	*	ns	**	ns	**	ns
	Drug	****	****	****	****	****	****

Mean scores represent $n = 6$ rats/group with the total being the average of the sum of all scores.

Means were compared by two-way analysis of variance where $P < 0.05$ (*), < 0.01 (**), < 0.001 (***), < 0.0001 (****).

evaluated over 6 h. Relative to healthy rats, NASH rats displayed a 77% increase from 0.97 to 1.67 $\mu\text{g}/\text{mL}\cdot\text{min}$ per gram bodyweight in plasma CDDP exposure as measured by $\text{AUC}_{0-\infty}$ (Table 4). This was consistent with a significantly different CDDP PK profile in NASH rats, relative to healthy rats, where the plasma concentration–time curve shifted upwards ($P = 0.0101$, two-way ANOVA, Fig. 3). Bodyweight normalized peak plasma CDDP concentrations over this time period also increased in NASH-induced rats from 22.9 ± 8.0 to 55.2 ± 17.2 $\mu\text{g}/\text{mL}/\text{g}$ bodyweight. These changes to plasma PK were accompanied by a reduction in plasma clearance of approximately 40% from 6.78 to 4.04 mL/min in NASH rats. Additionally, mean renal clearance and secretion rates were reduced in NASH by approximately half from 7.39 to 3.83 mL/min, relative to healthy rats (Table 2). NASH induced a slight, but non-significant reduction in GFR measured by plasma iothexol clearance when compared to healthy rats (Table 4). Over the 6 h collection interval, the total fraction of the CDDP dose excreted into urine did not differ significantly between healthy and NASH rats ($P = 0.8624$, two-way ANOVA, Fig. 3). However,

total tissue bound CDDP as a percentage of dose was reduced by approximately 15% in NASH rats, relative to healthy rats (Fig. 4). Conversely, NASH rats accumulated approximately 250% more total CDDP as a percentage of dose in liver tissue, relative to healthy rats (Fig. 4).

3.3. Expression of drug transporters is altered during NASH

To probe molecular mechanisms of altered CDDP PK and disposition, hepatic and renal drug transporter expression was evaluated in healthy and NASH rats used for these studies. Absolute drug transporter abundance was quantified by surrogate peptide LC–MS/MS. In renal plasma membrane protein fractions CTR1, a basolateral CDDP uptake transporter, decreased from 0.49 to 0.35 pmol/mg protein in NASH rats whereas OCT2 increased by a similar amount from 0.92 to 1.21 pmol/mg protein, relative to healthy rats (Fig. 5A). CDDP uptake transporters, OCT1 and OCT3, and vesicular transporter, ATP7A, did not change in kidney tissue. Expression of ATP7B, a vesicular transporting protein that removes the CDDP from the cytosol,

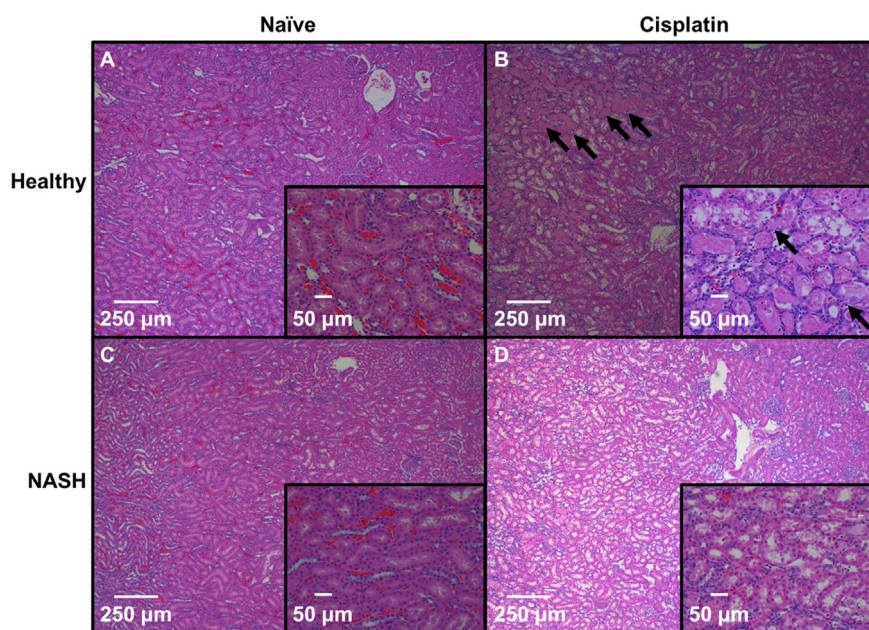


Figure 2 Histological kidney lesions were reduced in the proximal tubule of NASH rats. Representative images of H&E-stained kidney slices at 40 × and 200 × (insert) magnification. (A) Mid-cortex with glomeruli and more superficial cortex of naïve healthy rats at right and proximal convoluted tubules of deep cortex at left (40 ×). (B) There was mild to moderate degeneration and necrosis of convoluted tubules in more distal regions of tubules (arrows) mildly distended by cellular debris and proteinaceous material in CDDP control rats. There were mild increases in perivascular and extracellular matrix inflammation including lymphocytes and lesser numbers of macrophages (scattered blue foci between and rimming tubules). (C) Mid-to deep image of cortex with glomeruli and more superficial cortex at right and proximal convoluted tubules of deep cortex at left in NASH naïve rats. (D) Minimal degeneration and necrosis of tubular epithelial cells was present in the more distal regions of the proximal convoluted tubules in CDDP NASH rats. This image depicts minimal distension of tubules and minimal increases in extracellular matrix inflammation including few lymphocytes.

increased from 0.12 to 0.17 pmol/mg protein. Renal basolateral CDDP efflux proteins, MRP2, MRP4, MATE1, and P-gp, did not change significantly in animals induced with NASH, relative to healthy rats (Fig. 5A). Concurrent with elevated CDDP accumulation in NASH rats (Fig. 4), expression of sinusoidal CDDP uptake transporter OCT1 increased from 0.66 to 1.99 pmol/mg protein (Fig. 5B), although CTR1, OCT2, nor ATP7A or 7B did not change. This finding coincided with a reduction of MATE1, a canalicular membrane CDDP efflux transporter, in NASH rats from 0.25 to 0.13 pmol/mg protein, relative to healthy rats (Fig. 5B), whereas hepatic MRP4 expression increased slightly.

4. Discussion

The findings in this study suggest that functional alterations to elimination pathways induced by NASH elicit changes to CDDP PK, yielding a modest protective effect at the major target tissue of toxicity, the renal proximal tubule cell (Fig. 2, Table 2). This study also suggests that the observed reduction in CDDP renal clearance is likely a result of the sum of multiple elimination pathways: reduced renal filtration, reduced renal secretion, and increased hepatic uptake of CDDP. Furthermore, while the observed decrease in renal accumulation of CDDP (Fig. 4) coincides with a modest reduction in nephrotoxicity (Table 2), the

Table 3 Liver histopathological scoring of healthy and NASH rats receiving either CDDP or vehicle.

Disease	Drug	Total	Lipid accumulation	Necrosis	Apoptosis	Inflammation	Fibrosis	Biliary hyperplasia
Control	Naïve	0	0	0	0	0	0	0
	CDDP	0	0.17 ± 0.41	0	0	0	0	0
NASH	Naïve	2.33 ± 0.52	3.50 ± 0.55	0.83 ± 0.41	0.33 ± 0.52	1.67 ± 0.52	0.33 ± 0.52	1.50 ± 1.05
	CDDP	1.80 ± 0.45	2.80 ± 0.45	0.40 ± 0.55	0.80 ± 0.45	1.60 ± 0.55	0	1.40 ± 0.55
Two-way ANOVA	Diet	****	****	***	***	****	ns	****
	Drug	ns	ns	ns	ns	ns	ns	ns

Mean scores represent $n = 6$ rats/group with the total being the average of the sum of all scores.

Means were compared by two-way analysis of variance where $P < 0.05$ (*), < 0.01 (**), < 0.001 (***), < 0.0001 (****).

Table 4 CDDP pharmacokinetic parameters in healthy and NASH rats.

Index	Unit	Healthy	NASH
AUC _{0-∞}	μg·min/ (mL·g BW)	0.94 ± 0.26	1.67 ± 0.67*
AUC _{extrap}	%	10.23 ± 4.32	7.13 ± 2.62
Plasma CL	mL/min	6.78 ± 1.84	4.04 ± 1.53*
C _{max}	mg/(mL·g BW)	23.9 ± 8.0	55.2 ± 17.2*
Total urinary excretion	% of dose	94.35 ± 28.49	91.76 ± 17.86
CL _R	mL/min	7.39 ± 3.97	3.83 ± 1.01*
GFR	mL/min	1.64 ± 0.86	1.03 ± 0.44
Renal secretion	mL/min	6.23 ± 3.78	2.80 ± 0.93*

Non-compartmental PK parameters were calculated for each individual animal and means ($n = 6$ animals/group) were compared by Student's *t*-test where $P < 0.05$ (*).

opposite, but more robust increase in hepatic accumulation of CDDP during NASH (Fig. 4) is not correlated to any drug-related changes in hepatotoxicity (Table 3, Fig. 2).

Previous studies have demonstrated that free CDDP is quickly cleared and is highly plasma protein bound^{23,24}. Nephrotoxicity following acute CDDP exposure is proportional to peak plasma platinum concentration; as such, higher acute systemic exposure is predicted to manifest in enhanced toxicity²⁵. Indeed, this delayed toxic response in the kidney after acute CDDP exposure has been demonstrated in rodent models²⁶, yet, in the present study we observed a larger C_{max} (55.2 versus 23.9 μg/mL/kg BW) and plasma AUC in NASH rats, relative to healthy rats (Fig. 3, Table 4). Despite high peak and overall plasma CDDP concentrations in NASH rats, specific molecular mechanisms may attenuate nephrotoxicity—namely, reduced CDDP exposure at the proximal convoluted tubule.

Expression of OCT2, which is involved in CDDP uptake from the blood into cells, increases slightly in kidney tissue of NASH rats, which would increase CDDP uptake into the proximal convoluted tubule cells thereby increasing CDDP renal secretion and tissue accumulation (Fig. 5A). However, this effect may be negated by a similar decrease in CTR1 expression in NASH rats, as this transporter also transports CDDP into the proximal convoluted tubule cell. CDDP uptake by CTR1 is equilibrative

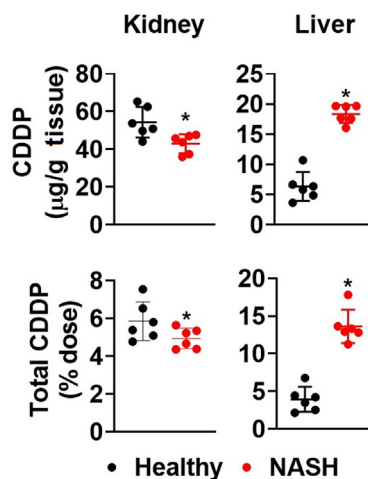


Figure 4 NASH reduces renal and enhances hepatic accumulation of CDDP. Rats in the PK cohort were sacrificed at 6 h and kidney and liver CDDP was quantified by LC–MS/MS with derivatization and normalized to dose. Scatter plots represent individual animals with mean values (horizontal lines) ± standard deviation of $n = 6$ animals/group. Differences in mean values were determined by unpaired, two-tailed Student's *t*-test where $P < 0.05$ (*).

whereas OCT2 is concentrative¹⁰, suggesting that increased OCT2 expression may predominate CDDP transport in favor of uptake. However, both transporters show relatively similar affinities for CDDP with K_m values of approximately 17 and 11 μmol/L for human OCT2 and CTR1, respectively^{27,28}. Reported maximal uptake capacity, measured by V_{max} for human OCT2 and CTR1 are 13.7 and 117 pmol/mg protein/min, respectively, suggesting that CTR1 may serve as a higher-capacity CDDP uptake transporter^{28,29}. Although comparative kinetics of these rat isoforms has not been evaluated, both human and rat CTR1 and OCT2 share 90% and 82% sequence homology, respectively, suggesting that these orthologs may function similarly. Taken together with the current study, these observations suggest that the reduction in renal CTR1 may functionally outweigh the increases in OCT2, thereby reducing CDDP secretion into the nephron and subsequent toxicity (Table 2, Fig. 4). Finally, ATP7B, which sequesters and removes copper and other substrates including CDDP from cells³⁰, was induced

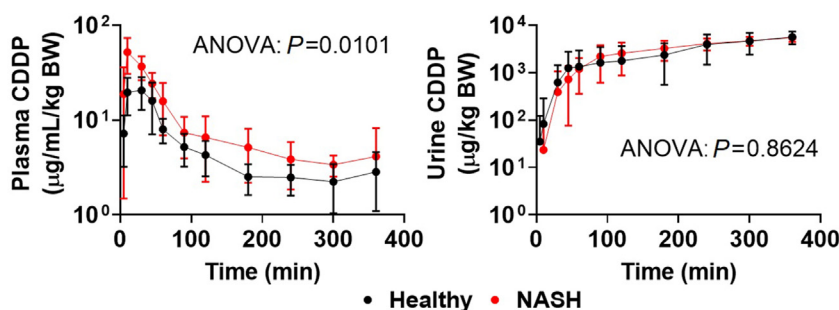


Figure 3 CDDP plasma and renal clearance is reduced in NASH-induced rats. In a separate cohort of healthy or NASH rats dosed with CDDP (6 mg/kg, i.p.), bodyweight-normalized plasma CDDP concentrations (left panel) and cumulative CDDP excreted into urine (right panel) was measured over 6 h. NASH rats did not display any significant increases in CDDP at any distinct timepoint, although a significant disease-dependent upward trend was observed. Conversely, bodyweight normalized total CDDP excreted into the urine did not differ between the two groups. PK curves were compared by two-way ANOVA with Sidak's *post-hoc* test.

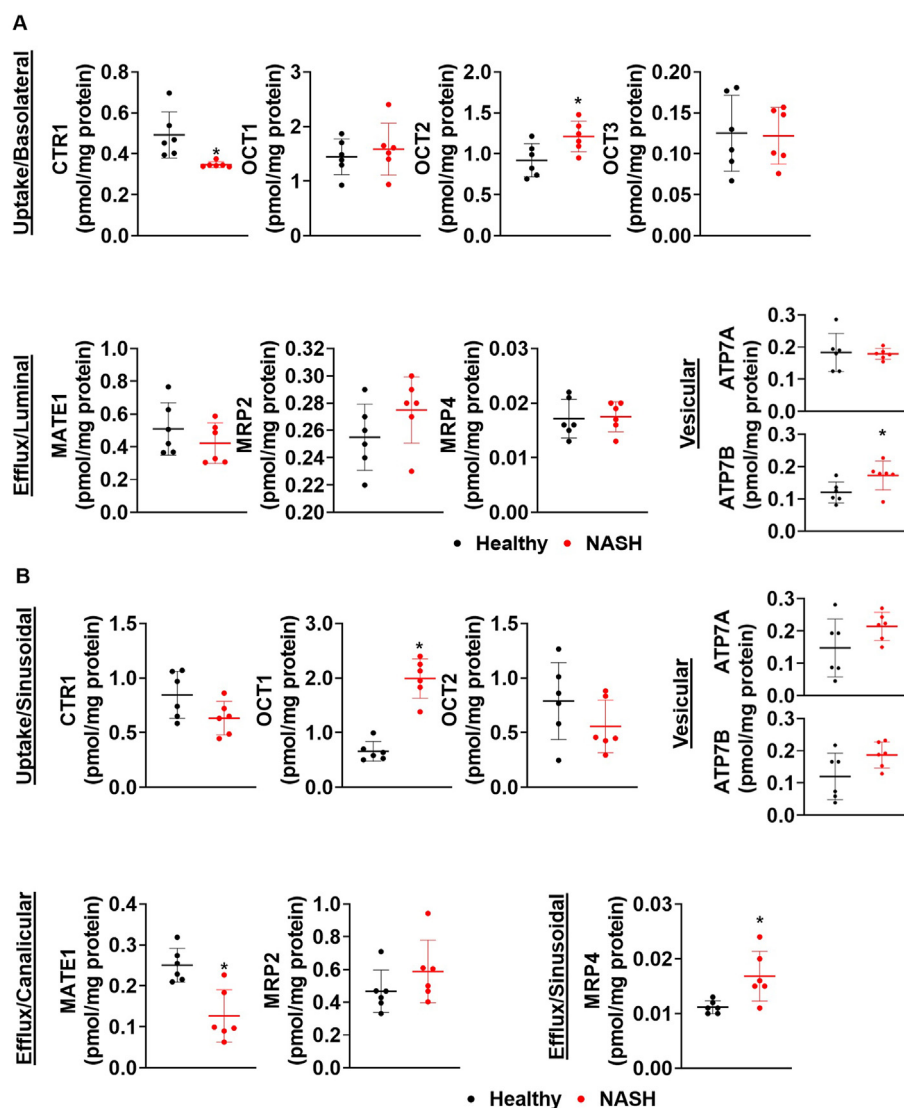


Figure 5 Expression patterns of CDDP renal and hepatic transporters are altered in NASH-induced rats. Secretory pathways in the proximal convoluted tubule and hepatocytes by substrate-specific transporters were quantified by surrogate peptide LC–MS/MS. (A) NASH rats exhibited reduced uptake (CTR1) and increased efflux (OCT2) transporter expression at the basolateral (blood) side of the proximal convoluted tubule, relative to healthy rats. Vesicular CDDP-transporter, ATP7B, increased significantly in NASH rats, relative to control. (B) Expression of hepatic CDDP uptake transporter, OCT1, on the sinusoidal membrane increased significantly in NASH rats, whereas expression of CDDP efflux transporter, MATE1, on the canalicular membrane decreased, relative to healthy rats. Scatter plots represent individual animals with mean values (horizontal lines) \pm standard deviation of $n = 6$ animals/group. Differences in mean values were determined by unpaired, two-tailed Student's *t*-test where $P < 0.05$ (*).

slightly in NASH kidney tissue, but not liver tissue (Fig. 5A). Increased ATP7B is associated with cancer cell resistance to CDDP and induction during NASH may offer an insight into a protective mechanism against toxicity in the proximal convoluted tubule cells^{31,32}. However, the directionality of ATP7-mediated CDDP removal into either the proximal convoluted tubule lumen or blood is not known, suggesting that this may not provide a mechanistic explanation for reduced CDDP systemic and renal clearance³³.

Notably, renal clearance is the sum of multiple processes, including filtration, reabsorption, and secretion at distinct locations along the nephron. Recently, disruptions to this physiological process have been documented in patients with NASH, despite the disease primarily manifesting in the liver¹². This includes reductions to GFR in both humans and animal models of NASH¹⁶,

which was partially recapitulated by this study, although at a non-significant level (Table 4). Over 6 h, the total amount of CDDP eliminated into the urine does not vary between healthy and NASH animals, suggesting that changes to total renal elimination of CDDP are minimal. However, the amount of CDDP and rate at which CDDP that is presented to the proximal convoluted tubule cells is reduced in NASH rats (Fig. 4, Table 4). This may be partially explained by reduced GFR, and subsequent blood flow to the kidney, thereby reducing renal CDDP disposition. Furthermore, temporal CDDP sequestration in the liver may also reduce renal clearance (Fig. 4).

While alterations to drug transporters within the proximal convoluted tubule may contribute to reduced renal clearance and renal secretion of CDDP, this study suggests that hepatic drug transport may also contribute to changes in renal CDDP PK.

CDDP is known to be mainly eliminated into the urine, with a very small amount being secreted into bile²³, although CDDP accumulates to comparable levels in both kidney and liver³⁴. Unexpectedly, we observed a robust increase of accumulated hepatic CDDP from approximately 5%–15% of the dose in NASH rats, relative to healthy rats (Fig. 4). These data suggest that a significant amount may be taken up into the liver, relative to healthy animals, which may contribute to the observed reduction in total body clearance. Indeed, hepatic OCT1 is highly induced in NASH rats and MATE1 expression decreases significantly (Fig. 5B). Although this study did not evaluate CDDP concentrations in bile or feces, these data do suggest that enhanced retention of CDDP in the liver may contribute to a reduction in renal clearance. Furthermore, no hepatic drug-induced histopathological lesions were found in CDDP-treated rats, relative to naïve rats (Table 3); CDDP-induced hepatotoxicity is rare and generally only presents following very high exposure, supporting this finding³⁵. While these data do not suggest an exhaustive mechanism of reduced renal exposure to CDDP, the data presented in this study provides a strong correlation between the NASH phenotype and decreased nephrotoxicity in NASH rats.

5. Conclusions

The data presented in this manuscript provide evidence for extrahepatic alterations to ADME and associate toxicity during NASH. Additionally, this study adds evidence demonstrating tissue specific toxicity caused by cisplatin.

Acknowledgments

This work was supported by the National Institutes of Health (R01ES028668, P30ES006694, and T32ES007091, USA).

Author contributions

Conceptualization: Joseph L. Jilek and Nathan J. Cherrington; Methodology: Joseph L. Jilek and Nathan J. Cherrington; Validation: Joseph L. Jilek; Formal analysis: Joseph L. Jilek, Michael Goedken, and Nathan J. Cherrington; Investigation: Joseph L. Jilek, Kayla L. Frost, Kevyn A. Jacobus, Wenxi He, and Erica L. Toth; Resources: Nathan J. Cherrington; Data curation: Nathan J. Cherrington and Nathan J. Cherrington; Writing—original draft preparation: Joseph L. Jilek, Michael Goedken, and Nathan J. Cherrington; Writing—review&editing: Joseph L. Jilek, Kayla L. Frost, Kevyn A. Jacobus, Wenxi He, Erica L. Toth, Michael Goedken, and Nathan J. Cherrington; Visualization: Joseph L. Jilek; Supervision: Nathan J. Cherrington; Project administration: Joseph L. Jilek and Nathan J. Cherrington; Funding acquisition: Nathan J. Cherrington.

Conflicts of interest

The authors declare no conflict of interest.

References

- Barabas K, Milner R, Lurie D, Adin C. Cisplatin: a review of toxicities and therapeutic applications. *Vet Comp Oncol* 2008;**6**:1–18.
- Ishida S, Lee J, Thiele DJ, Herskowitz I. Uptake of the anticancer drug cisplatin mediated by the copper transporter Ctr 1 in yeast and mammals. *Proc Natl Acad Sci U S A* 2002;**99**:14298–302.
- Filipski KK, Mathijssen RH, Mikkelsen TS, Schinkel AH, Sparreboom A. Contribution of organic cation transporter 2 (OCT2) to cisplatin-induced nephrotoxicity. *Clin Pharmacol Ther* 2009;**86**:396–402.
- Lin X, Okuda T, Holzer A, Howell SB. The copper transporter CTR1 regulates cisplatin uptake in *Saccharomyces cerevisiae*. *Mol Pharmacol* 2002;**62**:1154–9.
- Townsend DM, Deng M, Zhang L, Lapus MG, Hanigan MH. Metabolism of cisplatin to a nephrotoxin in proximal tubule cells. *J Am Soc Nephrol* 2003;**14**:1–10.
- Mitchell AE, Morin D, Lakritz J, Jones AD. Quantitative profiling of tissue- and gender-related expression of glutathione S-transferase isoenzymes in the mouse. *Biochem J* 1997;**325**:207–16.
- Sadzuka Y, Shimizu Y, Takino Y, Hirota S. Protection against cisplatin-induced nephrotoxicity in the rat by inducers and an inhibitor of glutathione S-transferase. *Biochem Pharmacol* 1994;**48**:453–9.
- Townsend DM, Tew KD, He L, King JB, Hanigan MH. Role of glutathione S-transferase Pi in cisplatin-induced nephrotoxicity. *Bio-med Pharmacother* 2009;**63**:79–85.
- Yonezawa A, Inui K. Importance of the multidrug and toxin extrusion MATE/SLC47A family to pharmacokinetics, pharmacodynamic/toxicodynamics and pharmacogenomics. *Br J Pharmacol* 2011;**164**:1817–25.
- Yonezawa A, Inui K. Organic cation transporter OCT/SLC22A and H⁺/organic cation antiporter MATE/SLC47A are key molecules for nephrotoxicity of platinum agents. *Biochem Pharmacol* 2011;**81**:563–8.
- Hamaguchi K, Godwin AK, Yakushiji M, O'Dwyer PJ, Ozols RF, Hamilton TC. Cross-resistance to diverse drugs is associated with primary cisplatin resistance in ovarian cancer cell lines. *Cancer Res* 1993;**53**:5225–32.
- Targher G, Bertolini L, Rodella S, Lippi G, Zoppini G, Chonchol M. Relationship between kidney function and liver histology in subjects with nonalcoholic steatohepatitis. *Clin J Am Soc Nephrol* 2010;**5**:2166–71.
- Shah RR, Smith RL. Addressing phenoconversion: the Achilles' heel of personalized medicine. *Br J Clin Pharmacol* 2015;**79**:222–40.
- Canet MJ, Hardwick RN, Lake AD, Dzierlenga AL, Clarke JD, Goedken MJ, Cherrington NJ. Renal xenobiotic transporter expression is altered in multiple experimental models of nonalcoholic steatohepatitis. *Drug Metab Dispos* 2015;**43**:266–72.
- Clarke JD, Dzierlenga AL, Nelson NR, Li H, Werts S, Goedken MJ, Cherrington NJ. Mechanism of altered metformin distribution in nonalcoholic steatohepatitis. *Diabetes* 2015;**64**:3305–13.
- Laho T, Clarke JD, Dzierlenga AL, Li H, Klein DM, Goedken M, Micuda S, Cherrington NJ. Effect of nonalcoholic steatohepatitis on renal filtration and secretion of adefovir. *Biochem Pharmacol* 2016;**115**:144–51.
- Canet MJ, Hardwick RN, Lake AD, Dzierlenga AL, Clarke JD, Cherrington NJ. Modeling human nonalcoholic steatohepatitis-associated changes in drug transporter expression using experimental rodent models. *Drug Metab Dispos* 2014;**42**:586–95.
- Thakkar N, Slizgi JR, Brouwer KLR. Effect of liver disease on hepatic transporter expression and function. *J Pharm Sci* 2017;**106**:2282–94.
- Oda M, Koyanagi S, Tsurudome Y, Kanemitsu T, Matsunaga N, Ohdo S. Renal circadian clock regulates the dosing-time dependency of cisplatin-induced nephrotoxicity in mice. *Mol Pharmacol* 2014;**85**:715–22.
- Dobyan DC, Levi J, Jacobs C, Kosek J, Weiner MW. Mechanism of cis-platinum nephrotoxicity: II. Morphologic observations. *J Pharmacol Exp Therapeut* 1980;**213**:551–6.
- Shaik AN, Altomare DA, Lesko LJ, Trame MN. Development and validation of a LC–MS/MS assay for quantification of cisplatin in rat plasma and urine. *J Chromatogr B Analyt Technol Biomed Life Sci* 2017;**1046**:243–9.
- Turner ME, Laverty KJ, Jeronimo PS, Kaufmann M, Jones G, White CA, Holden RM, Adams MA. Validation of a routine two-sample iohexol plasma clearance assessment of GFR and an

- evaluation of common endogenous markers in a rat model of CKD. *Phys Rep* 2017;**5**:e13205.
23. Siddik ZH, Newell DR, Boxall FE, Harrap KR. The comparative pharmacokinetics of carboplatin and cisplatin in mice and rats. *Biochem Pharmacol* 1987;**36**:1925–32.
 24. Hanada K, Ninomiya K, Ogata H. Pharmacokinetics and toxicodynamics of cisplatin and its metabolites in rats: relationship between renal handling and nephrotoxicity of cisplatin. *J Pharm Pharmacol* 2000;**52**:1345–53.
 25. Campbell AB, Kalman SM, Jacobs C. Plasma platinum levels: relationship to cisplatin dose and nephrotoxicity. *Cancer Treat Rep* 1983;**67**:169–72.
 26. Perše M, Večerić-Haler Ž. Cisplatin-induced rodent model of kidney injury: characteristics and challenges. *BioMed Res Int* 2018;**2018**:1462802.
 27. Filipiński KK, Loos WJ, Verweij J, Sparreboom A. Interaction of Cisplatin with the human organic cation transporter 2. *Clin Cancer Res* 2008;**14**:3875–80.
 28. Liang ZD, Stockton D, Savaraj N, Tien Kuo M. Mechanistic comparison of human high-affinity copper transporter 1-mediated transport between copper ion and cisplatin. *Mol Pharmacol* 2009;**76**:843–53.
 29. Sprowl JA, Ciarimboli G, Lancaster CS, Giovino H, Gibson AA, Du G, Janke LJ, Cavaletti G, Shields AF, Sparreboom A. Oxaliplatin-induced neurotoxicity is dependent on the organic cation transporter OCT2. *Proc Natl Acad Sci U S A* 2013;**110**:11199–204.
 30. Safaei R, Otani S, Larson BJ, Rasmussen ML, Howell SB. Transport of cisplatin by the copper efflux transporter ATP7B. *Mol Pharmacol* 2008;**73**:461–8.
 31. Komatsu M, Sumizawa T, Mutoh M, Chen ZS, Terada K, Furukawa T, Yang XL, Gao H, Miura N, Sugiyama T, Akiyama S. Copper-transporting P-type adenosine triphosphatase (ATP7B) is associated with cisplatin resistance. *Cancer Res* 2000;**60**:1312–6.
 32. Katano K, Safaei R, Samimi G, Holzer A, Rochdi M, Howell SB. The copper export pump ATP7B modulates the cellular pharmacology of carboplatin in ovarian carcinoma cells. *Mol Pharmacol* 2003;**64**:466–73.
 33. Ciarimboli G. Membrane transporters as mediators of Cisplatin effects and side effects. *Sci Tech Rep (Cairo)* 2012;**2012**:473829.
 34. Stewart DJ, Benjamin RS, Luna M, Feun L, Caprioli R, Seifert W, Loo TL. Human tissue distribution of platinum after *cis*-diamminedichloroplatinum. *Cancer Chemother Pharmacol* 1982;**10**:51–4.
 35. Cavalli F, Tschopp L, Sonntag RW, Zimmermann A. A case of liver toxicity following *cis*-dichlorodiammineplatinum(II) treatment. *Cancer Treat Rep* 1978;**62**:2125–6.